Microbial Cell Factories

RESEARCH Open Access

Manufacturing of the highly active thermophile PETases PHL7 and PHL7mut3 using *Escherichia coli*

Lisa Fohler[1], Lukas Leibetseder[1], Monika Cserjan-Puschmann[1] and Gerald Striedner[1*]

Abstract

Background The global plastic waste crisis requires combined recycling strategies. One approach, enzymatic degradation of PET waste into monomers, followed by re-polymerization, offers a circular economy solution. However, challenges remain in producing sufficient amounts of highly active PET-degrading enzymes without costly downstream processes.

Results Using the growth-decoupled enGenes e^X-press V2 *E. coli* strain, pH, induction strength and feed rate were varied in a factorial-based optimization approach, to find the best-suited production conditions for the PHL7 enzyme. This led to a 40% increase in activity of the fermentation supernatant. Optimization of the expression construct resulted in a further 4-fold activity gain. Finally, the identified improvements were applied to the production of the more active and temperature stable enzyme variant, PHL7mut3. The unpurified fermentation supernatant of the PHL7mut3 fermentation was able to completely degrade our PET film sample after 16 h of incubation at 70 °C at an enzyme loading of only 0.32 mg enzyme per g of PET.

Conclusions In this research, we present an optimized process for the extracellular production of thermophile and highly active PETases PHL7 and PHL7mut3, eliminating the need for costly purification steps. These advancements support large-scale enzymatic recycling, contributing to solving the global plastic waste crisis.

Keywords PET degradation, PETase, Recycling, Enzyme production, *E. coli*, PHL7, Bioreactor cultivation

Background

Polyethylene terephthalate (PET), the world's most widely used polyester plastic, was first patented in 1941 in England [1, 2]. Ten years later the US company DuPont started working with the material, patenting the first PET bottle in 1973 [3]. Rapidly the production of PET fibers, films, bottles and containers expanded globally, with nowadays 83 million metric tons of PET being produced per year, and rising [4, 5]. Only a fraction of this amount is reused or recycled while a large percentage is incinerated or accumulated in landfills [6]. To combat the frightening amount of built-up PET waste, every known recycling strategy must be exploited, aided by the development of novel approaches. Currently, mechanical and chemical PET recycling are the most commonly employed techniques in industry. While mechanical recycling is relatively cost-effective it has the main disadvantage of reducing the product quality significantly [7]. Chemical recycling on the other hand, has many advantages over mechanical recycling, but depending on the

*Correspondence:
Gerald Striedner
gerald.striedner@boku.ac.at
[1]Institute of Bioprocess Science and Engineering, BOKU University, Muthgasse 18, Vienna 1190, Austria

used method, can require high pressure, temperature and create impurities during the depolymerization process [8]. In recent years, a new and promising recycling method emerged: enzymatic depolymerization of PET to its monomers terephthalic acid (TPA) and ethylene glycol (EG). This approach allows the targeted breakdown of PET under normal pressure and relatively mild temperatures without the need for toxic chemicals or even pure, pre-sorted PET waste. The obtained monomers can then be used for re-polymerization to PET without a loss of quality, making true circular PET economy possible [9, 10]. As promising as this sounds, enzymatic recycling is facing a few challenges of its own. The slow enzymatic conversion rates and the difficulty of producing highly active PET degrading enzymes in a cost-effective process have so far impeded implementation on a larger scale [11].

Enzymes recognized for their ability to degrade PET are, among others, leaf-branch compost cutinase (LCC), *Humicola insolens* cutinase (HiC), *Ideonella sakaiensis* PETase (IsPETase), *Thermobifida fusca* hydrolase (TfH) and *Thermobifida fusca* cutinases (TfCut1 and TfCut2). Soong et al. [12] describe complete degradation of a low crystallinity PET film (lcPET) in 72 h using LCC as an enzyme, while HiC reached full degradation in 96 h [13]. IsPETase was stated to degrade 1.5% of lcPET in 24 h, which would indicate complete degradation in 66 days (linear degradation rate assumed) [14]. Müller et al. [15] report 54% weight loss of a lcPET film in 3 weeks with TfH and TfCut2 degrades 17% of lcPET in 50 h, by extrapolation resulting in ~12 days for full degradation [16]. In 2022, a new PET degrading enzyme, polyester hydrolyse Leipzig 7 (PHL7), was found by Sonnendecker et al. [17]. This highly active enzyme has a denaturation temperature of 79 °C, which enables fast recycling at elevated temperatures. The glass-transition temperature of PET, roughly 70 °C, enhances the polymer chain mobility, thereby rendering the chemical bonds more accessible to the enzyme. Thus, enzymatic stability at temperatures around 70 °C for prolonged periods of time is an important factor for efficient enzymatic PET recycling. Even though LCC, the most promising enzyme for PET recycling before the discovery of PHL7, has a 5 °C higher denaturation temperature, the activity of PHL7 surpasses that of LCC by far. The novel polyester hydrolase is described to fully degrade a lcPET film in 16 h, outperforming all other enzymes mentioned above distinctly. Due to systematic mutagenesis of specific residues in the PHL7 subsites I and II, Richter et al. [18] were able to enhance the PHL7 performance even further, creating a PHL7 triple mutant (PHL7mut3 or PHL7_Q175E, L210T, D233K) with a higher denaturation temperature and 1.3-fold increased activity.

In the past, only very low expression titers of cutinases, PETases and related enzymes were achieved, amounting to only a few milligrams of product per liter [19–24]. A possible reason for this may be the cytotoxic nature of these enzymes, causing cell lysis, excessive foaming during fermentation and challenges in downstream operations [25, 26]. Y. Tan et al. [27]described the tendency of cutinases to degrade both the inner and outer membrane of *E. coli*, leading to release of the enzyme into the extracellular space even without the use of a signal sequence. Extracellular expression due to cell lysis can prove advantageous, as it eliminates the need for the homogenization step. However, the adverse effects of cell lysis like low titers, foaming and highly viscous cell broths, must be dealt with for the process to become feasible. This might be the reason why a large percentage of the PETase expression experiments described in literature were done in shake flasks and not in reactors [28–32]. Certainly, expression conditions gathered from shake flask experiments cannot be used to implement large scale enzyme production, thus an optimized process for a highly active PET degrading enzyme developed under controlled conditions is required. Ideally, the cell-free supernatant of the fermentation broth after centrifugation could be diluted and utilized in the recycling process without the necessity of any purification steps, to keep costs as low as possible. However, due to inhibitory effects of cell compounds like DNA and host cell proteins released into the fermentation medium together with the enzyme, purification is often essential to ensure sufficient enzyme performance. Therefore, a process optimization strategy should not only focus on achieving the highest enzyme titers but more importantly on the volumetric enzyme activity in the unpurified fermentation supernatant. The enzyme titer, the release of protein into the supernatant and the enzyme inhibition by compounds present in the fermentation supernatant all influence the volumetric activity. By identifying the fermentation process yielding the highest volumetric activity the most beneficial combination of those factors can be found. Preceding the process optimization, the expression strain and expression construct have to be selected. As an expression host *E. coli* has, *inter alia*, the advantages of fast growth, short process durations, inexpensive media components and a vast molecular toolbox to work with [33]. In 2020 a new, growth-decoupled *E. coli* strain, enGenes e^X-press V2, was created and published by Stargardt et al. [34]. This host has two major advantages, increased resources for recombinant protein production and enhanced extracellular expression, making it the ideal chassis for our project. The phage T7 Gp2 gene is under control of the pBAD promoter system, which can be induced by addition of arabinose to the fermentation medium. After induction the expressed Gp2 protein inhibits the *E. coli* host

cell RNA polymerase. The cell growth is halted, freeing up cellular resources for increased recombinant protein production. Due to cellular aging in the course of the fermentation process cell membranes become permeable, furthering the release of protein of interest (POI) into the extracellular space. With the deletion of the arabinose operon genes *araBADC* arabinose metabolization is prevented, rendering low inducer concentrations sufficient. Recombinant protein production is induced by the addition of IPTG but for a gentler induction strategy, arabinose can be used as an inducer for both growth decoupling and POI expression. This effect was attributed to promoter cross-talk and leads to slower but prolonged expression, which can yield a higher overall titer with certain POIs [35]. Additionally, facilitating soluble, extracellular expression the gene of interest (GOI) can be cloned in an expression vector equipped with a N-terminal lamB signal sequence to redirect the product to the periplasmic space [36] and a T7A3 tag. The T7A3 tag is a polypeptide with a large net negative charge, promoting soluble expression and in combination with certain POIs can also increase the product titer and therefore act as an expression enhancer [37, 38]. In the development stage it can also be beneficial to attach an affinity tag to the protein of interest for easier analytics and the preparation of a purified standard of the product. The use of a hexa-histidine (His) tag finds widespread applicability as antibodies for the detection in analytics are readily available and purification over nickel-nitrilotriacetic acid (Ni-NTA) columns is relatively quick and easy in lab scale [39, 40]. Those aspects considered, we chose our host strain and expression cassette accordingly aiming to find an enzyme production process yielding highly active enzyme solutions with little or no need of further purification.

Methods

Strains and cloning

The chemically competent *E. coli* strain NEB5α (New England Biolabs, NEB, Ipswitch, MA, USA), was used for plasmid amplification. The electrocompetent *E. coli* strain e^x-press V2 (enGenes Biotech, Vienna, Austria) was employed for recombinant protein expression. Transformation of the generated plasmids into the respective host organisms was done according to the manufacturer's instructions. The PHL7 and PHL7mut3 enzyme sequences (see supplementary information S3) were codon optimized for *E. coli* with a codon optimizer online tool (OPTIMIZER, Universitat Rovira i Virgili, http://genomes.urv.es/OPTIMIZER/) and ordered as gBlocks from Integrated DNA Technologies (IDT, Coralville, IA, USA). The PHL7 enzyme gBlock was ordered with the N-terminal T7A3 sequence and the C-terminal 6xHis-tag already attached, whereas the PHL7mut3 enzyme was ordered without the T7A3 sequence. As a backbone an in-house produced pET30a.cer expression vector was used [41]. The cloning procedures were performed using the Q5® High-Fidelity DNA Polymerase and restriction enzymes provided by NEB following the supplier's guidelines. A table with all used primers and templates is presented below (Table 1), the primer and gBlock sequences are listed in the supplementary information (S2 and S3). All construct sequences were confirmed by Sanger sequencing.

Fed-batch bioreactor cultivations for enzyme production

To optimize our three selected critical process parameters (CPPs), induction strength, feed rate and pH, we first designed an initial fermentation process. This experimental set-up was kept consistent over all experiments, except for the variation in the three CPPS.

For the pre-culture, a 500 mL baffled bottom flask was filled with 30 mL of semi-synthetic medium containing

Table 1 All used primers and templates for the cloning of the expression constructs used in this work

Expression construct	PCR product	Primer 1	Primer 2	Template
pET30a.*cer*_ spa_T7A3_PHL7_His	Backbone	pET30a.*cer* _sense	NdeI_pET30a.*cer*_new_as	pET30a.*cer*
	Insert	BsaI_T7A3_ spa_sense	PHL7_His_as	T7A3_PHL7_His (gBlock)
pET30a.*cer*_ lamB_T7A3_PHL7_His	Leader was swapped with overhang primers	lamB2_ pET30a.*cer* _sense	lamB1_ pET30a.*cer* _as	pET30a.cer_ spa_T7A3_PHL7_His
pET30a.*cer*_ lamB_PHL7_His	Backbone was amplified without T7A3 tag	pET30a.*cer*_ lamB_as	PHL7_sense	pET30a.*cer*_ lamB_T7A3_PHL7_His
pET30a.*cer*_ T7A3_PHL7_His	Backbone was amplified without lamB leader	pET30a.*cer*_ as	T7A3_sense	pET30a.*cer*_ lamB_T7A3_PHL7_His
pET30a.*cer*_ PHL7_His	Backbone was amplified without T7A3 tag and lamb leader	pET30a.*cer*_ as	PHL7_sense	pET30a.*cer*_ lamB^{S}T7A3_PHL7_His
pET30a.*cer*_ PHL7mut3_His	Backbone	NdeI_ pET30a.*cer* _ new_as	BsaI_Tzenit_ sense	pET30a.*cer*_PHL7_His
	Insert	HEG sense	HEG as	PHL7mut3_His (gBlock)

50 µg/mL kanamycin. The medium was inoculated with 2 mL of working cell bank and incubated for 5 h at 37 °C and 200 rpm. The optical density (OD) was measured and the amount of cell suspension equaling 25 OD units was used to inoculate 500 mL of batch medium (see supplementary information S1) in the DASGIP reactor system (Eppendorf SE, Hamburg, Germany). The temperature was kept at 37 (+/- 0.2) °C, the pH control was set to 7 (+/- 0.1) and regulated by dosing 12.5% ammonia solution. The dissolved oxygen (DO) cascade was designed to maintain the DO at 30% by first accelerating the stirrer speed (400–1200 rpm), then increasing the air flow rate (10–200 sL/h) and finally increasing the oxygen concentration in the gas flow (21–100%). Foaming in the reactor was kept under control by dosing antifoam agent (1:10 diluted, Struktol J673A, Schill+Seilacher, Böblingen, Germany) when needed. The batch phase ended after 8.25 h with a cell dry weight (CDW) of 10 g/L. Then the first feed phase was started, which was an exponential feed (feed medium composition see supplementary information S1) with a growth rate of 0.135 h-1. At the end of the exponential feed phase 40 g/L of CDW were reached. Subsequently the feed was set to a linear feed profile with fixed feed rate (0.08 g glucose/min in the initial fermentation process) and the temperature was set to 30 °C. With the start of the linear feed, the growth of the host cells was halted by addition of 10 mM arabinose to express the T7 phage protein Gp2 and in parallel the enzyme expression was induced with IPTG (0.4 µmol/g CDW in the initial fermentation process) thereby decoupling growth and recombinant protein production. The first sample was taken right before induction as a reference and to determine possible basal expression of PHL7. Further samples were drawn every two hours for a maximum of ten hours. In fermentation runs that showed heavy foaming early on, sampling intervals were shortened to one hour.

This initial fermentation process was the template for all our process optimization trials. For the initial and extended informed design experiments we exclusively varied the three CPPs according to Figures below.

As described in the previous section fermentation run 1 represents the initial fermentation process before optimization. This run was performed in biological triplicates to determine the variability of the collected experimental data. All subsequent runs were analyzed in technical triplicates. All collected samples were analyzed using the methods explained below.

Enzyme activity assay – TPA release

The drawn fermentation samples were centrifuged at 14,000 rpm for 10 min to separate the cells from the fermentation medium. For every sample 5 safe lock reaction tubes (1.5 mL, Eppendorf) were prepared, 4 of which were filled with an 8 mg PET film (ES30-FM-000145, Goodfellow Cambridge Ltd, UK), and one was left empty to function as a blank. The supernatant was diluted 1:7.5 in 1 M potassium phosphate buffer pH 8 and 0.5 mL were added to each of the prepared reaction tubes. After incubating the tubes for 3 h at 70 °C and 700 rpm the absorption at 242 nm was measured in a microplate reader (Tecan Infinite M200). If the absorption exceeded a value of 3 the samples were diluted in potassium phosphate buffer. To obtain the terephthalic acid concentration from the absorption values, a calibration curve for the range of 9.375 to 600 µM TPA was set up. The slope of our calibration curve was 0.0036. The mM TPA released was calculated according to Eq. (1).

$$mM TPA\,released\,in\,3h = \frac{Abs._{242nm}(sample) - Abs._{242nm}(blank)}{0.0036\,(slope) * 1000\,(conv.\,\mu M\,to\,mM)} * dil.\,factor \quad (1)$$

To rule out any TPA release of the PET film in buffer, six 1.5 ml reaction tubes containing solely 1 M potassium phosphate buffer and six reaction tubes containing the buffer and PET film were incubated for 3 h at 70 °C and subsequently the absorbance at 242 nm was measured. The comparison of the absorbance of buffer and buffer with PET film can be found in supplementary information S4. Enzyme activity assay – weight loss of PET film.

Standardized goodfellow PET film was wiped with ethanol to remove residues from the surface. To generate PET samples as an enzyme substrate, 8 mg discs were punched out with a hole puncher. The selected fermentation supernatant samples were diluted 1:7.5 in 1 M potassium phosphate buffer (pH 8) and 0.5 mL were added to the reaction tubes containing the PET discs. After incubating the reaction tubes at 70 °C and 700 rpm in a temperature controlled shaker (VWR® thermal shaker lite) the remaining PET samples were removed, washed, dried and weighed. The incubation time was 72 h for the samples of the initial factorial-based optimization study- and 24 h for the expression construct evaluation samples. The % of PET film degraded was calculated according to Eq. (2).

$$\%\,PET\,degradation = \frac{weight\,of\,PET\,film\,after\,assay - PET\,film\,start\,weight}{PET\,film\,start\,weight} * 100 \quad (2)$$

To rule out any weight loss of the PET film in buffer without enzyme, six 2 ml reaction tubes containing 1 M potassium phosphate buffer and pre-weighed PET film were incubated for 20 h at 70 °C and subsequently washed, dried and weighed. The results of these blank measurements can be found in supplementary information S5.

Cell disruption and inclusion body solubilization

For cell disruption a 1 mg pellet sample was obtained by measuring the optical density at 600 nm and calculating the needed amount of cell suspension (OD_{600}/CDW [g/L]=3.5). After centrifugation (10 min, 14000 rpm), we obtained a supernatant and a cell pellet fraction. The cell pellets were resuspended in 400 µl sonication buffer (30 mM TRIS, 50mM NaCl, pH7.2) chilled on ice and disrupted by sonication (Hielscher UP100H, 2×90 s, amplitude: 70%, cycle time: 0.5 s). The cell debris and insoluble fraction were removed by centrifugation (10 min, 14000 rpm) and the supernatant (intracellular soluble fraction) was transferred to a fresh tube. The remaining pellet was washed twice (100 mM TRIS-HCl pH8) and subsequently the IBs were solubilized in 8 M urea solution for 30 min under mild shaking at room temperature. After a last centrifugation step (10 min,14000 rpm) the supernatant, now containing the solubilized IB fraction, was transferred to a fresh tube. In total we obtained 3 fractions per sample, the fermentation supernatant, the intracellular soluble and the inclusion body fraction.

SDS-PAGE

To estimate the concentration of POI in our samples as well as the distribution between the three fractions (inclusion body, intra- and extracellular soluble) the samples were analyzed via sodium dodecyl sulfate-polyacrylamide gel electrophoresis (SDS-PAGE) as described by Stargardt et al. [34]. Bovine serum albumin (BSA) standards with concentrations of 25, 50 and 75 µg/mL were used for product titer estimations. For visualization of the protein bands Coomassie Brilliant blue R250 was used. To couple the band intensity to a protein concentration, the BSA standard bands as well as the POI bands were analyzed densitometrically with the ImageQuantTL 1D software (Version 8.2.0).

Determination of DNA concentration in the fermentation supernatant

DNA found outside of the cell, in the fermentation medium, is always evidence of cell lysis. The severity of the lysis can be estimated by determination of the DNA concentration, which we did using the Invitrogen™ Qubit™ dsDNA Quantification Assay Kit following the manufacturers guidelines. Measurements were performed using the Qubit™ 4 Fluorometer (Thermo Fisher Scientific).

Results

Design of expression constructs

All factorial-based optimization experiments were carried out using the enGenes e^X-press V2 production strain, harboring a pET30a.cer plasmid containing the lamB_T7A3_PHL7_His expression construct. To promote extracellular expression the lamB signal sequence was employed to direct our enzyme into the periplasmic space, from where the protein can be released into the supernatant more easily, due to effects of outer membrane leakiness [42] and cell lysis. The T7A3 tag was utilized to enhance soluble expression and overall expression levels. For easier analysis and purification during the optimization phase of the process, we included a C-terminal hexa-histidine tag in our expression construct. Later results showed the need to examine the influence of each tag element on its own. Therefore, we generated three further expression constructs, lamB_PHL7_His, T7A3_PHL7_His and PHL7_His (see Table 2). For the expression of the PHL7mut3 enzyme variant we cloned the PHL7mut3_His construct.

Table 2 Expression constructs and abbreviations used in further experiments

Abbreviation	Expression construct
Control	lamB – T7A3 – PHL7 – His
lamB	lamB – PHL7 – His
T7A3	T7A3 – PHL7 – His
PHL7	PHL7 – His
PHL7mut3	PHL7mut3 – His

Production of extracellular PHL7 in bioreactor cultivations

Initial factorial-based optimization study

For the fed-batch cultivations in benchtop bioreactors the three critical process parameters (CPPs) – pH, induction strength and feed rate – were varied in three levels, generating a design space with 27 experiments to cover all combinations. Reducing the number of experiments, we pursued a 2-level full factorial design approach with 11 fermentation runs, the 8 corner points of our design space and the center point, which was run in triplicate (see Fig. 1C). Through the course of fermentation offline samples were taken for the determination of enzymatic terephthalic acid (TPA) release, DNA content in the supernatant and cell dry weight. A standardized PET film was incubated with diluted fermentation supernatant at 70 °C for 3 h and the concentration of released TPA monomers was measured at 240 nm. This value was taken as a measure of enzyme activity.

Measuring the DNA concentration in the supernatant of the fermentation broth gave insight on the level of cell lysis (see Fig. 1D). The high levels of DNA in the supernatant of our fermentations indicated a toxicity of our POI on the expression strain and lead to high viscosity of the samples. We also observed low separation efficiency of cells and supernatant through centrifugation.

Coinciding with the DNA content measurements of the supernatant samples were, apart from runs 2 and 3, the TPA release measurements. In run 3, the fermentation

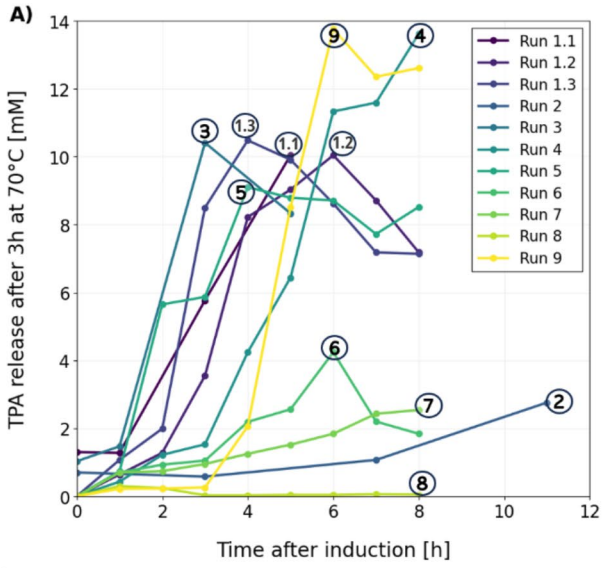

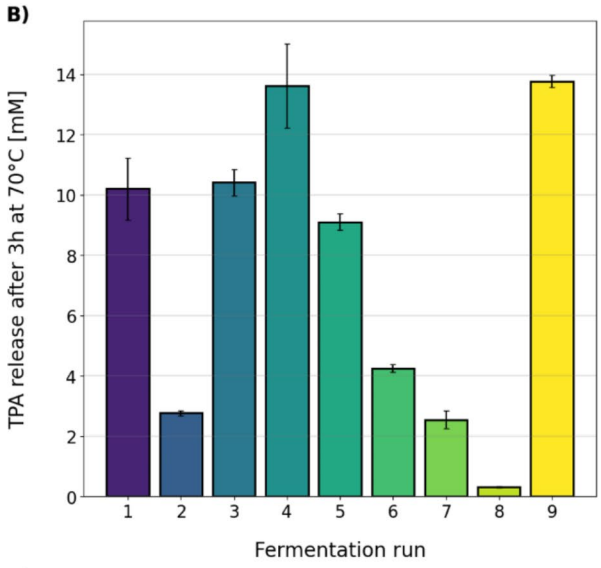

C)

Ferm. run	Ind. strength* [µmol IPTG/g CDW]	pH	Feed rate [g glucose/min.]
1 (3x)	0.4	7.0	0.08
2	0.0	6.5	0.04
3	0.8	7.5	0.12
4	0.8	6.5	0.04
5	0.8	7.5	0.04
6	0.0	7.5	0.04
7	0.0	7.5	0.12
8	0.0	6.5	0.12
9	0.8	6.5	0.12

* + 10 mM arabinose in all fermentations

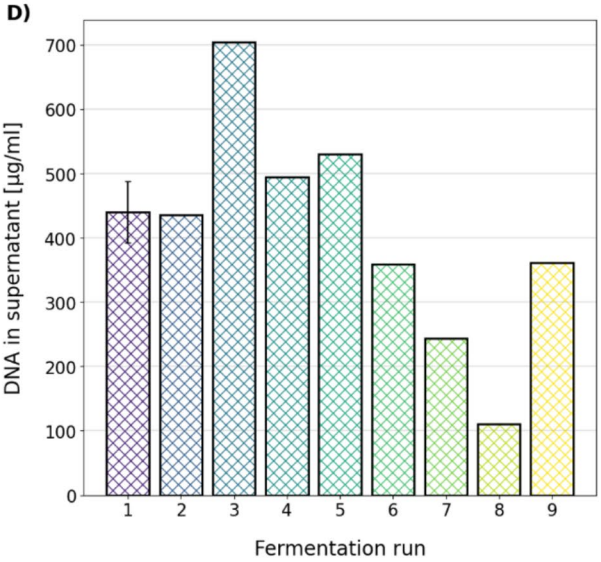

Fig. 1 Initial factorial-based optimization study, **A**: activity of each experimental run in the course of the fermentation (after induction), run 1 was carried out in triplicate, **B**: highest recorded activity of each experimental run, error bar of run 1 calculated from biological and technical replicates and of runs 2–9 from technical replicates, **C**: experimental set-up of all fermentation runs, **D**: DNA concentration in the fermentation supernatant of each experiment at time of highest activity, error bar of run 1 calculated from two biological replicates, no replicates of runs 2-9

with all CPPs at their highest level, the highest DNA content was recorded. This level of lysis was not matched by a superior enzyme activity. Experiment 2 on the other hand, run at the lowest CPP levels, shows an unexpectedly high DNA concentration. The TPA release (i.e. activity) over the course of each fermentation run can be seen in Fig. 1A, the highest achieved activity of each individual run is plotted in Fig. 1B. The fermentation experiments 2, 6, 7 and 8 were induced by the addition of arabinose only. Supernatants of those four fermentations showed the lowest activities in the design space. By far the highest activity was achieved by supernatants of fermentation runs 4 and 9, which both were conducted at low pH (6.5) and high induction strength (0.8 µmol IPTG/g CDW). The only difference between those two fermentations was the feed rate, which was low in run 4 and high in experiment 9. These findings raised the question whether an even lower pH and even higher induction strength would result in further improvement of activity. Therefore, the design space was extended to include pH6 and an induction strength of 1.2 µmol IPTG/g CDW. The feed rate was not extended to include a further level, as this parameter showed little influence.

Extended factorial-based optimization study

The center point (1) and the two best performing experiments 4 and 9 of the initial design space were accompanied by eight further fermentations (points A - H) to form the extended design space (see Fig. 2C). As in the previous set of experiments, Fig. 2A shows the activity of the supernatant samples over the course of the production phase, whereas Fig. 2B only depicts the best performing sample of each fermentation run, regardless of the time this activity maximum was reached.

Fermentation supernatants of fermentation runs 4, 9 and A were the only ones surpassing a TPA release of 12 mM in 3 h, with all other samples falling beneath that value. All three fermentations were conducted at the same pH of 6.5 and the same induction strength of 0.8 µmol IPTG/g CDW, with just the feed rate diverging. Fermentation supernatants of experiments D and E, which were both obtained of fermentations carried out at pH 6 and an induction strength of 0.4 µmol IPTG/g CDW, showed the lowest activity in the extended design space. A combination of lowest pH and highest induction strength (runs C and F) yielded an improvement of the activity in the supernatant compared to runs D and E but did not outperform the fermentations at pH 6.5 and an induction strength of 0.8 µmol IPTG/g CDW. The highest DNA content in the supernatant was measured at the lowest tested pH, feed rate and induction strength, respectively, (see Fig. 2D, run D). Interestingly, the highest DNA content was not recorded at a combination of the highest levels of pH, induction strength and feed rate (run H) but at the intermediate level (run A).

Additionally, PET films were incubated with diluted fermentation supernatants of four different fermentation runs for 72 h at 70 °C and the weight loss was determined (instead of TPA release after 3 h). The first four runs of the extended factorial-based optimization study were chosen for this comparison and as Fig. 3 shows, the fermentation supernatant of experiment A was able to fully degrade the PET sample in the given time, while runs B, C and D only yielded 71, 54 and 43% degradation, respectively.

Influence of construct elements on expression an activity

Even though the factorial-based optimization study with the first expression construct lamB_T7A3_PHL7_His (control) lead to significant improvements of the fermentation supernatant's activity, still a large part of the enzyme was produced in inclusion bodies (IBs, see Fig. 4C). To evaluate the contribution of each part of our expression construct, lamB_PHL7_His (lamB), T7A3_PHL7_His (T7A3) and PHL7_His (PHL7) constructs were cloned, expressed in 2 L benchtop reactors and compared to the control. The influence of the C-terminal His-tag was investigated in previous experiments and no negative impact on either expression or activity was found (data not shown). The lamB signal sequence was employed to direct the POI into the periplasmic space with the goal to promote the release of the enzyme into the supernatant, as extracellular production is preferred. Unfortunately, the effect of the signal sequence was a strong inclusion body formation and very little soluble enzyme production (see Fig. 4A+C). The same effect was also observed with other signal sequences such as the post translational ompA and pelB sequences, as well as the co-translational dsbA sequence (data not shown). Omitting the signal sequence resulted in complete soluble POI expression, without any inclusion body formation. Still, extracellular production was achieved, due to a combination of the use of the growth decoupled enGenes e^X-press V2 strain and the cell toxic nature of the POI. The supernatants of all four constructs were diluted and incubated together with a PET film sample at 70 °C for 20 h. The supernatant of the PHL7 construct without the lamB leader and the T7A3 tag was able to fully degrade the PET film, whereas lamB, T7A3 and the control only achieved 48, 97 and 87% respectively (see Fig. 5).

The minimal difference in degradation efficiency between T7A3 and PHL7 (3%) suggests only a modest influence of the N-terminal tag. However, as the assay was concluded after 20 h without intermediate measurements, it is possible that PHL7 may have reached complete degradation significantly earlier. Under this assumption, the impact of the T7A3 tag on enzymatic

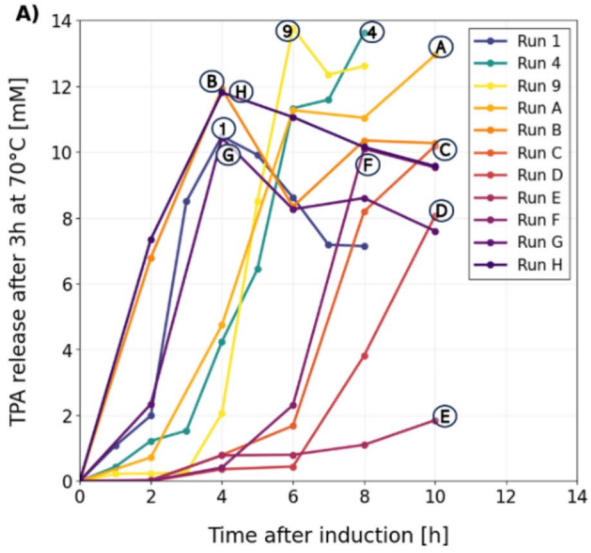

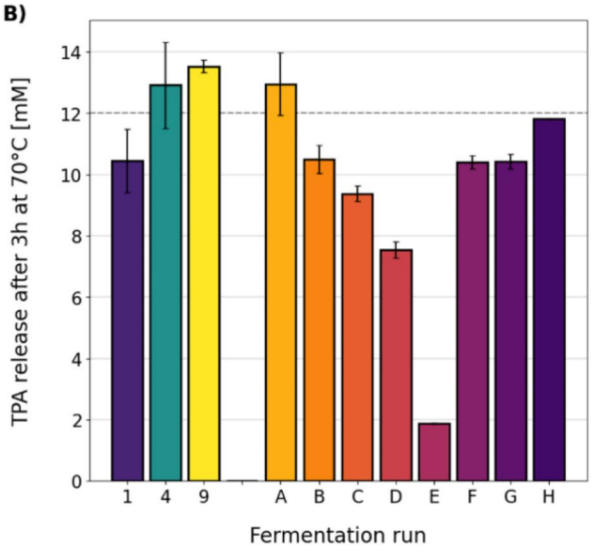

C)

Ferm. run	Ind. strength* [µmol IPTG/g CDW]	pH	Feed rate [g glucose/min.]
1 (3x)	0.4	7.0	0.08
4	0.8	6.5	0.04
9	0.8	6.5	0.12
A	0.8	6.5	0.08
B	1.2	7.0	0.08
C	1.2	6.0	0.08
D	0.4	6.0	0.04
E	0.4	6.0	0.12
F	1.2	6.0	0.04
G	0.4	7.0	0.04
H	1.2	7.0	0.12

* + 10 mM arabinose in all fermentations

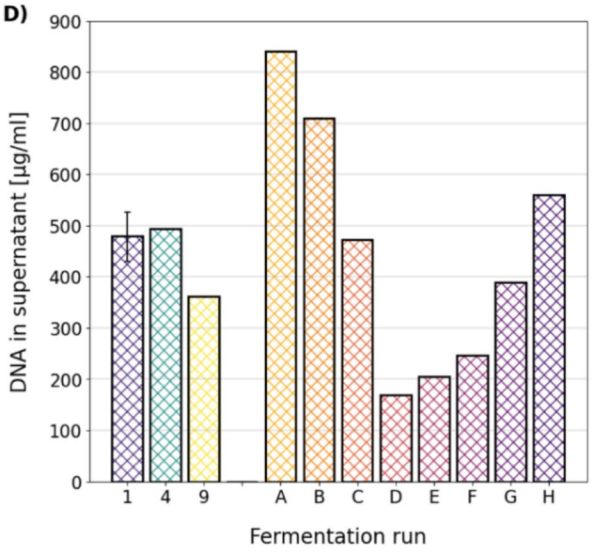

Fig. 2 Extended factorial-based optimization study, **A**: activity of each experimental run in the course of the fermentation (after induction) **B**: highest recorded activity of each experimental run, error bar of run 1 calculated from biological and technical replicates and of runs 4, 9 and A – H from technical replicates, **C**: experimental set-up of all fermentation runs, **D**: DNA concentration in the fermentation supernatant of each experiment at time of highest activity, error bar of run 1 calculated from two biological replicates, no replicates of runs 4, 9 and A - H

activity could be more substantial than the final degradation percentages indicate. The hypothesis that PHL7 achieved full degradation in less than 20 h is supported by subsequent experiments (see Figure below), where PHL7 fully degraded PET in 16 h at saturation conditions (which were also used in this experiment). While the lamB leader clearly has a huge (negative) impact on soluble expression (Fig. 4A+C), the T7A3 tag could impair the enzyme activity, as it is not cleaved off (Fig. 4B+C). The presence of the solubility tag at the N-terminus of the enzyme accounts for the significantly higher molecular weight bands observed in the T7A3 and control constructs compared to the lamB and PHL7 constructs. In any case, the PHL7 construct (Fig. 4D) with its completely soluble expression and superior performance in the weight loss assay, is the best candidate to proceed with.

Expression of optimized PHL7triple mutant (PHL7mut3)

In 2023 Richter et al. [18]. created a PHL7 variant (PHL7mut3) by introducing three point mutations to the PHL7 wild type sequence, which resulted in higher activity and temperature stability. PHL7mut3 was produced as PHL7mut3_His (see Table 2) under the optimized conditions determined for the PHL7 wild type. After 4 h of induction, a clear POI band was visible in the supernatant fraction on the SDS-PAGE gel (Fig. 6A+B, lane 7). The band intensity increased until the end of fermentation

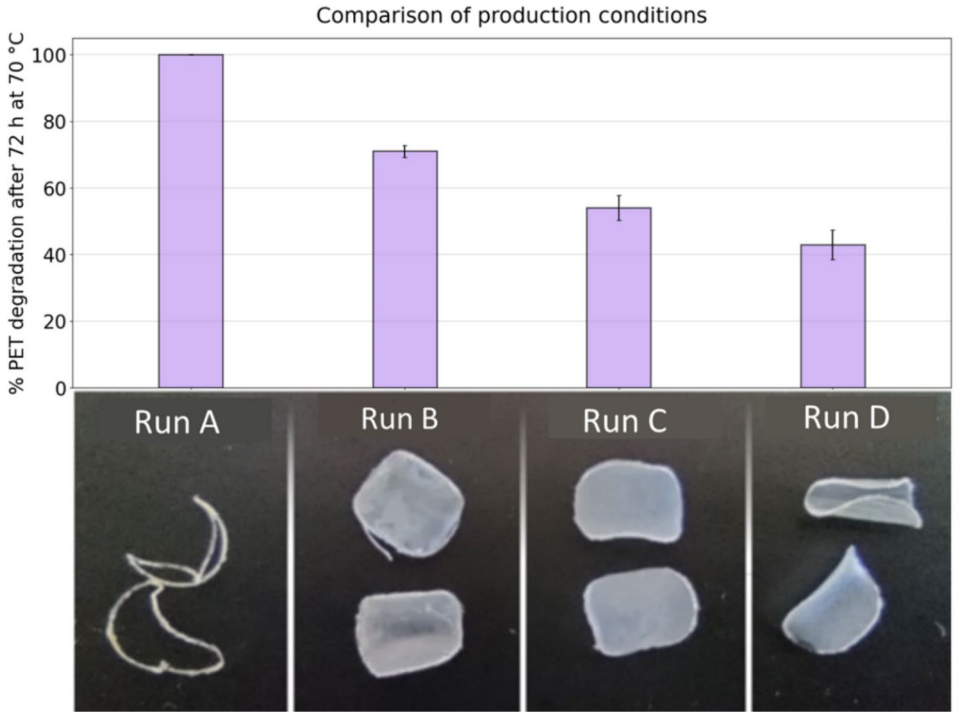

Fig. 3 Comparison of PET film degradation after 72 h incubation with diluted fermentation supernatants of runs A (100% degradation), B (71% degradation), C (54% degradation) and D (43% degradation) in 1 M potassium phosphate buffer, pH8 at 70 °C for 72 h; images of PET films were captured by camera

at 10 h of induction, where the maximum extracellular enzyme titer was reached. Many host cell proteins (HCP) were also visible (Fig. 6A), which indicated cell lysis. To purify the supernatant a heat precipitation step was performed. After incubating the solution at 72 °C for 10 min a majority of HCPs precipitated and were separated via centrifugation without a significant loss of the desired enzyme.

The comparison of purified enzyme standard and unpurified fermentation supernatant at different enzyme loadings is shown in Fig. 7. The initial construct (lamb_T7A3_PHL7_His), which was used for all factorial-based optimization fermentations, reached about 30% degradation in 16 h at an enzyme loading of 0.32 µg/mg PET. For the purified enzymes of both PHL7_His and PHL7mut3_His the saturation of the PET film surface was reached at 0.2 µg enzyme/mg PET and 100% degradation was reached after 16 h of incubation at 70 °C with this loading. Below the saturation point, PHL7mut3_His showed a slightly higher activity than PHL7. The corresponding unpurified fermentation supernatants show saturation at a marginally higher enzyme loading of 0.32 µg/mg PET but were still able to completely degrade the PET sample in 16 h. At an enzyme loading of 0.2 µg/mg PET the activity of the PHL7_His fermentation supernatant was decreased by about 20% compared to the purified standard, whereas the difference in activity between purified PHL7mut3_His and PHL7mut3_His from the fermentation supernatant was less pronounced.

Discussion

In this work we show the development of an optimized and scalable *E. coli* process, producing the highly active enzymes PHL7 and PHL7mut3. As we strived to optimize our process in a way that omits any purification steps, achieving the highest enzyme titer in combination with the highest enzyme activity is the goal. For the time-resolved fermentation analysis a lot of samples had to be processed, therefore the TPA release in 3 h was measured to compare the supernatants obtained from all fermentations at all sampling time points. All samples were diluted with the same dilution factor, which means that the values obtained from these assays are the result of the combined effects of enzyme titer and activity of the enzyme in the presence of potential inhibitory compounds. The TPA release assay was chosen over the widely used p-nitrophenyl butyrate (p-NPB) [43] assay with the argument of higher significance related to later applications. Measuring the DNA concentration in the supernatant of the fermentation broth gave insight on the level of cell lysis, which can be an important factor for downstream processing [37]. High concentrations of DNA in the supernatant lead to high viscosity, decreased centrifugation or filtration performance during separation of cells and fermentation supernatant and filter blockage during HPLC

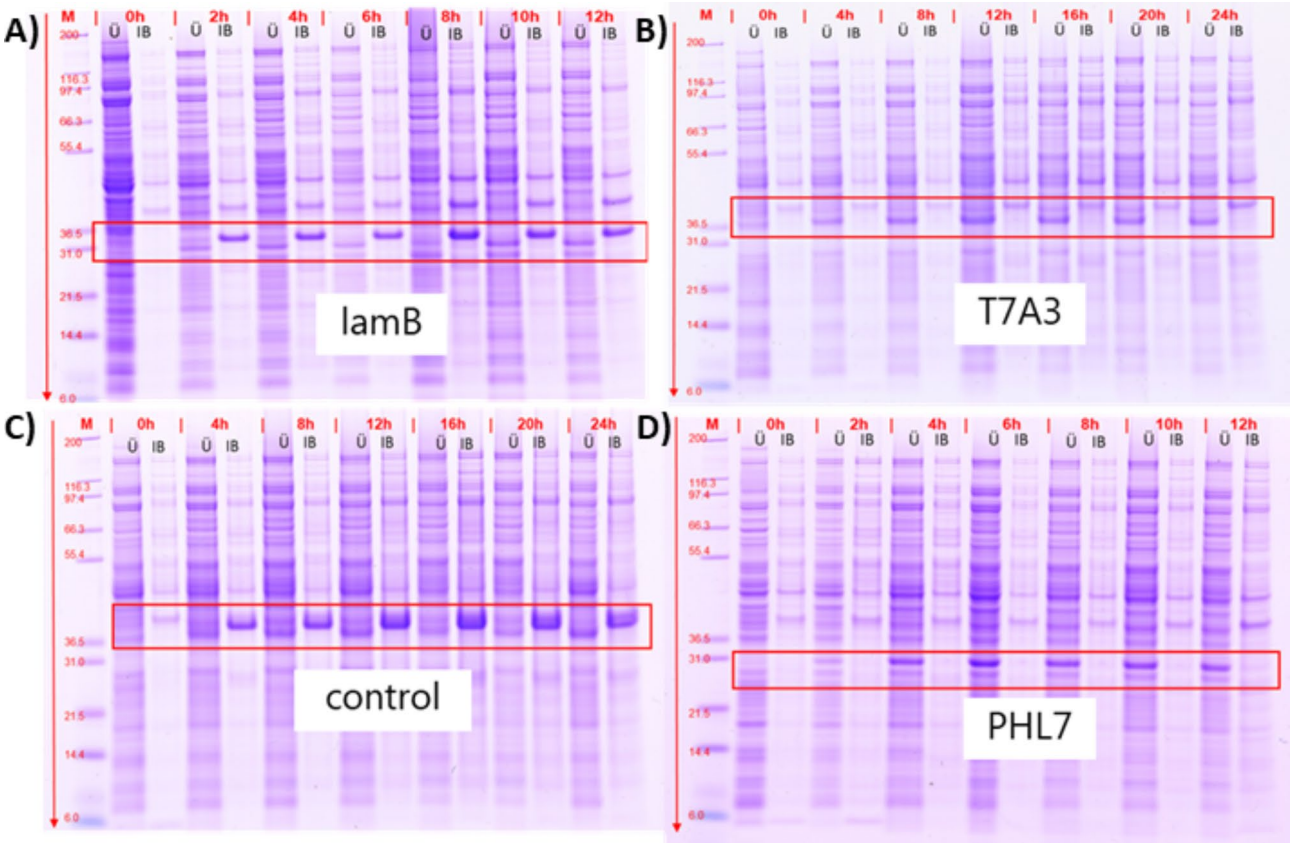

Fig. 4 Comparison of the soluble (Ü) and inclusion body (IB) fractions of fermentation samples of 4 different constructs; **A**: lamb: lamb_PHL7_His construct without T7A3 tag; **B**: T7A3: T7A3_PHL7_His construct without lamb leader; **C**: control: lamb_T7A3_PHL7_His construct (was used for factorial-based optimization study), **D**: PHL7: PHL7_His construct without lamb leader and T7A3 tag; samples were taken every 2 h for 12 h in total, starting at the point of induction

product analysis of samples. We observed a correlation between supernatant activity and DNA content, which is plausible because *E. coli* strains usually do not secret proteins and the release into the supernatant is therefore mostly governed by cell lysis. Effects like enzyme inhibition by other released compounds in the solution (HPCS, DNA, etc.) may interfere with this correlation, decreasing the expected activity. For this reason, the fermentation process was not optimized to achieve the highest enzyme titer but the highest activity in the supernatant.

In the initial factorial-based optimization design space, the fermentation supernatants of the runs 4 and 9 achieved a TPA release of 13.62 and 13.76 mM in 3 h, respectively. The supernatants of all other runs yielded below 12 mM TPA release. This clear improvement resulted from fermentations at the lowest tested pH and the highest tested induction strength, while the feed rate had no apparent influence. Therefore, the effect of an even lower pH and higher induction strength had to be assessed. Extending the design space by 8 further experiments secured the findings of the initial design space with the ideal production conditions of pH 6.5 and an induction strength of 0.8 µmol IPTG/g CDW.

The weight loss assays were then performed over a longer period of time with selected supernatant samples to show the differences in volumetric activity in a more tangible way. Comparing the TPA release data after 3 h of incubation, experiment 1 in the initial set of experiments showed a performance that was in between that of runs B and C of the extended set. In the 72 h weight loss assay experiments B and C showed 71 and 54% degradation, respectively, while the supernatant of run A yielded a fully degraded PET sample. Those results indicated a 40% improvement of the supernatant activity compared to the initial process. Despite all optimization efforts, insoluble enzyme expression made up a considerable amount of the recombinant protein production. Neither reduced induction strength nor a pH shift influenced the distribution between soluble and insoluble expression. Usually, lower fermentation temperatures are advised when it comes to shifting recombinant protein production towards soluble expression [44, 45]. As our production phases ran at 30 °C instead of 37 °C already and IB formation was still predominant, this strategy was clearly ineffective in this case. Therefore, the influence of the expression construct elements was evaluated individually. As the PHL7

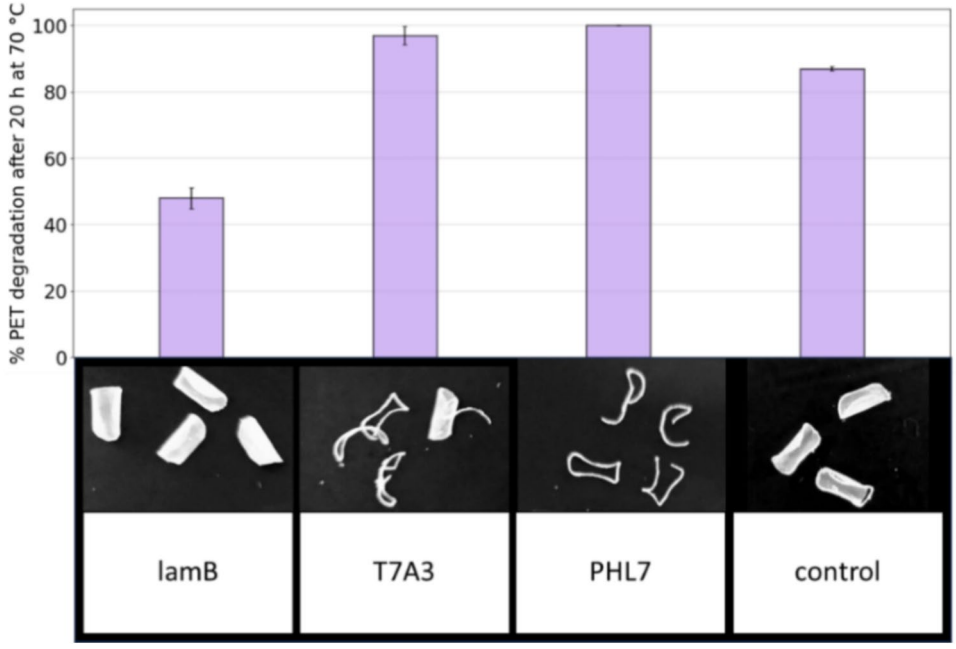

Fig. 5 Comparison of PET film degradation after incubation with 1:7.5 diluted fermentation supernatants of constructs lamB (48% degradation), T7A3 (97% degradation), PHL7 (100% degradation) and control (87% degradation) in 1 M KPO buffer, pH8 at 70 °C for 20 h; images of PET films were captured by camera

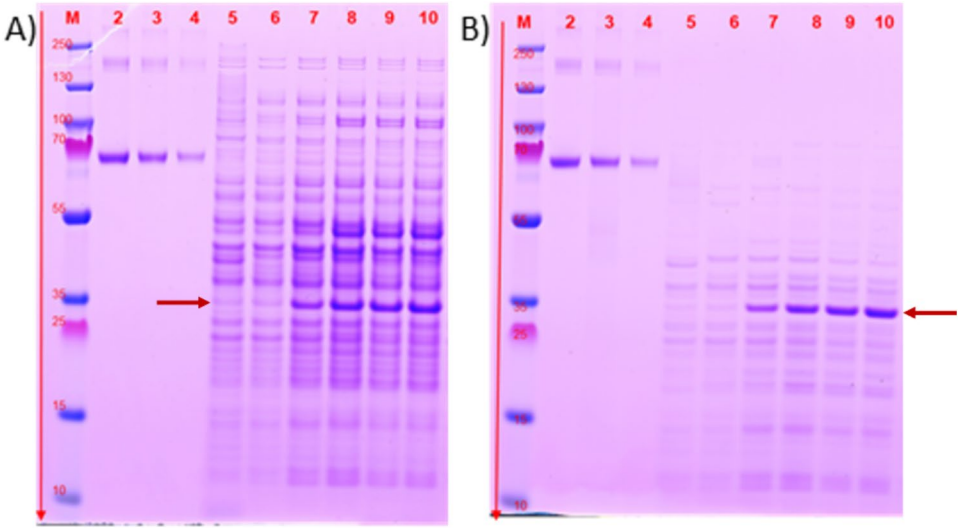

Fig. 6 **A**: lane 1: Thermo Scientific™ PageRuler™ Plus Prestained Protein Ladder, 10 to 250 kDa, lanes 2–4: Bovine serum albumin (BSA) standards with 75, 50 and 25 µg/ml, lanes 5–10: fermentation supernatant in the course of induction, 0 h (undiluted), 2 h (1:2 dil.), 4 h (1:2 dil.), 6 h (1:3 dil.), 8 h (1:5 dil.) and 10 h h (1:5 dil.) samples; **B**: as in A, but fermentation supernatant samples were purified by heat treated for 10 min. at 72 °C

enzyme possesses two cysteine residues, the necessity of a disulfide bond formation could be assumed. In *E. coli* this post-translational modification could only be achieved by the oxidizing environment of the periplasm, making a leader sequence an obvious choice to express this protein [46, 47]. Contrary to our assumptions we found that directing the POI to the periplasm via a signal sequence caused the inclusion body formation. Omitting the lamb leader and consequently shifting to cytosolic expression resulted in the production of soluble enzyme only. The second part of the construct to be evaluated was the T7A3 solubility tag, which can also function as an expression enhancer [37]. Unlike the signal sequence this tag is not cleaved off by the host organism, which can potentially influence the enzyme activity. Moreover, it alters the enzyme's molecular size, causing the POI to migrate a slightly shorter distance on the SDS-PAGE gel, aligning with HCP bands of our production strain. This

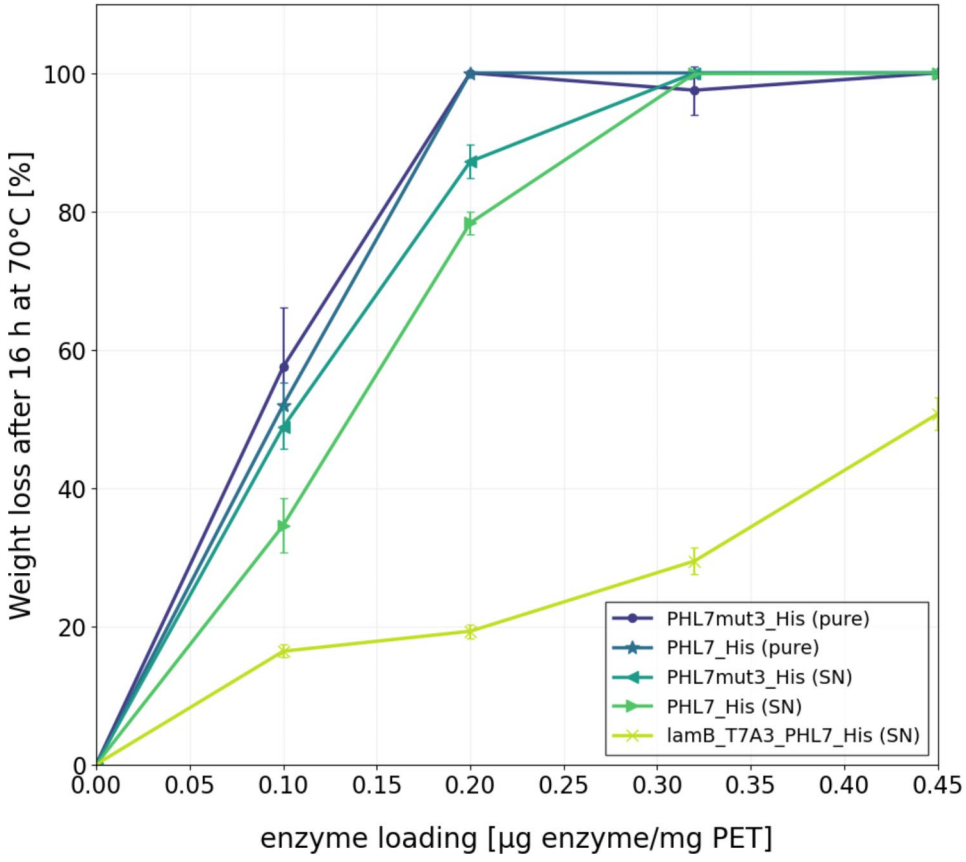

Fig. 7 Comparison of PET film degradation of purified PHL7_His standard and unpurified fermentation supernatants of the initial lamb_T7A3_PHL7_His and the optimized PHL7_His constructs, as well as purified PHL7mut3_His standard and unpurified PHL7mut3_His fermentation supernatants

effect might cause the impression that the soluble and inclusion body bands of the control in Fig. 4 are more pronounced than the ones of the lamB samples. In fact, the product bands of the control are partially obscured by the host cell protein bands, which was also confirmed by mass spectrometry. Taking into account these considerations, we observed no discernible impact of the T7A3 tag on either solubility or titer when combined with this specific POI. The enzyme activity, however, was slightly reduced. Those findings lead us to select the PHL7_His construct for all further experiments, as soluble expression of active enzyme was our goal. Compared to the lamb_T7A3_PHL7_His construct, the PHL7_His fermentation supernatant achieved 4-fold more PET degradation at an enzyme loading of 0.2 mg/g PET in the 16 h assay (Fig. 7). Lastly, the even more active and stable PHL7 triple mutant, PHL7mut3, was produced using the optimized expression construct and fermentation conditions. The maximum titer and activity in the supernatant were reached after 10 h of induction, rendering this a time-efficient process. Simple and inexpensive purification of the enzyme can be achieved by heat precipitation of the impurities at 72 °C. This treatment is highly effective to obtain a purer enzyme fraction without the loss of our product. At the stage of TPA recovery, a purer enzyme fraction is advantageous because it leads to cleaner and whiter TPA, facilitating easier repolymerization processes and ultimately enhancing the quality of PET. Also, heat purification and subsequent volume reduction or lyophilization can be beneficial when the enzyme has to be shipped to the recycling plant or stored for a prolonged period of time. As the comparison between purified PHL7mut3 and the fermentation supernatant in our 16 h degradation assay shows (see Fig. 7), at an enzyme loading of 0.2 mg enzyme/g PET the purification would only improve the activity by 10%. At an enzyme loading of 0.32 mg enzyme/g PET both the purified and the unpurified enzyme degrade the PET to 100%.

To meet the global demand of enzymes for PET recycling, highly active enzymes paired with a cheap, fast and efficient production process are key. The pitfalls for implementing enzymatic recycling in industry so far were rather low enzyme titers, hard to control production processes, the necessity of costly downstream operations and slow turnover numbers of the employed enzymes, which means very long degradation process times. H. Seo et al. [23]. reports a titer of 6.2 mg/L of IsPETase secreted into the fermentation supernatant, while X. Wang et al. [21].

Table 3 Overview of the reported activities of different PET degrading enzymes

Enzyme	Catalytic activities	Enzyme loading	Reference
PHL7	13 mM TPA monomers release in 3 h at 70 °C against gfPET film	0.2 mg/g PET	Shown in this paper
IsPETase	0.3 mM products released in 18 h at 30 °C against PET film	Not stated	[48]
Fast-PETase	33.8 mM products released in 96 h at 50 °C against gfPET film	~0.33 mg/g PET	[28]
HotPETase	6.07 mM soluble monomers in 5 h at 60 °C against cryPET	~3.5 mg/g PET	[29]
ThermoPETase	0.12 mM soluble monomers in 72 h at 40 °C against PET film (42% crystallinity)	~0.4 mg/g PET	[30]
BbPETase	0.8 mM soluble monomers in 3 days at 40 °C against mcPET (17% crystallinity)	Not stated	[31]
LCC	17.4 mM products released in 27 h at 72 °C	5.7 mg/g PET	[32]

mentioned 12 mg/L of IsPETase produced extracellularly. LCC titers are comparably low with 6–8 mg/L purified from 1 L of fermentation supernatant by S. Sulaiman et al. [22]. In this research we report extracellular titers of 400–500 mg/L of PHL7 and PHL7mut3. To put the findings of the TPA release assays into context, we compared our results with those stated in literature in Table 3 (see below). The only enzymes in this table that can to some extent compete with PHL7 (13 mM of monomers released in 3 h) are HotPETase (6.07 mM in 5 h) and LCC (17.4 mM in 27 h). However, despite enzyme loadings of 3.5 and 5.7 mg/g PET for HotPETase and LCC, respectively, a load over 17 times higher than with PHL7, their degradation performance was still inferior.

Conclusions

Utilizing a growth-decoupled bacterial host strain enabled resource-efficient enzyme expression. In the fed-batch experiments for PHL7 expression in benchtop reactors the combination pH6.5 and an induction strength of 0.8 µmol IPTG/g CDM yielded the fermentation supernatant with the highest activity. The feed rate showed negligible influence on the process. Evaluating the influence of our construct elements on enzyme expression and activity we showed that, in contrast to periplasmic expression, cytosolic expression solves the problem of inclusion body formation, while we were still able to achieve a release of our enzyme into the fermentation supernatant. The developed process was adopted for the production of PHL7mut3. The PHL7mut3 fermentation supernatant showed incredible PET degrading activity, with 100% degradation of a gfPET film in 16 h at an enzyme loading of only 0.32 mg/g PET. The combination of an enzyme as stable and capable as PHL7mut3 together with this fast, inexpensive and scalable production process is unmatched so far.

Still, a major issue in this production process is the effect of cell lysis and therefore high DNA content in the supernatant. Due to the high viscosity of the fermentation broth operations like centrifuging, filtering and separating the remaining cells and cell debris from the medium are next to impossible. As the fermentation supernatant is the product and should be easily obtained and processed, this is an issue that has yet to be solved.

To date, the majority of research in the field of enzymatic recycling focuses on enzyme engineering to generate more active and stable plastics degrading enzymes and undoubtedly this is a pressing topic but on the other hand it is just half the battle. If those discovered enzymes cannot be produced in economically feasible processes and in the amounts needed, those discoveries will never leave the research stage, as they can't be implemented by industry. For this reason, the process development for producing these enzymes plays a crucial role, that should not be underestimated.

Abbreviations

BSA	Bovine serum albumin
CDW	Cell dry weight
CPP	Critical process parameter
DO	Dissolved oxygen
E. coli	Escherichia coli
EG	Ethylene glycol
GOI	Gene of interest
HiC	Humicola insolens cutinase
His	Histidine
IB	Inclusion body
IPTG	Isopropyl ß-D-1-thiogalactopyranoside
IsPETase	Ideonella sakaiensis PETase
LCC	Leaf and branch compost cutinase
lcPET	Low crystallinity PET
Ni-NTA	Nickel-nitrilotriacetic acid
OD	Optical Density
PET	Polyethylene terephthalate
PHL7	Polyester hydrolase Leipzig 7
POI	Protein of interest
Rpm	Revolutions per minute
SDS-PAGE	Sodium dodecyl sulfate-polyacrylamide gel electrophoresis
sL	Standard liters
SSM	Semi-synthetic medium
TfCut	Thermobifida fusca cutinases
TfH	Thermobifida fusca hydrolase
TPA	Terephthalic acid

Supplementary Information

The online version contains supplementary material available at https://doi.org/10.1186/s12934-024-02551-6.

Supplementary Material 1

Supplementary Material 2

Acknowledgements
We gratefully acknowledge funding from the European Union's Horizon 2020 research and innovation program under grant agreement no. 887913 (ENZYCLE). We thank Dr. Christian Sonnendecker from the University of Leipzig, Germany, for providing the PHL7 and PHL7mut3 enzyme sequences used in this study.

Author contributions
G.S. conceived the general project idea. L.F. designed the experiments. L.F and L.L. performed the experiments. L.F. wrote the manuscript with support from L.L., G.S, and M.S. G.S. and M.C. supervised the project. All authors provided critical feedback and contributed to the writing of the manuscript.

Funding
The research in this article was part of the Enzycle Project, which has received funding from the Bio-based Industries Joint Undertaking (BBI JU) and the European Union's Horizon 2020 program under grant agreement nº887913.

Data availability
All data supporting the findings of this study are available within the paper and its Supplementary Information. Media compositions are provided in Supplementary Table S1, Sequence and primer information is provided in Supplementary Table S2 and S3. The PHL7 sequence is also accessible via PDB DOI: https://doi.org/10.2210/pdb7nei/pdb. A file containing all raw rata for this manuscript can be found under: https://doi.org/10.5281/zenodo.12167499.

Declarations

Ethics approval and consent to participate
Not applicable.

Consent for publication
The authors state that the manuscript is the author's original work and all authors mutually agree on submitting the manuscript.

Competing interests
The authors declare no competing interests.

Received: 12 July 2024 / Accepted: 30 September 2024
Published online: 10 October 2024

References

1. Liu C, Shi C, Zhu S, Wei R, Yin CC. Structural and functional characterization of polyethylene terephthalate hydrolase from Ideonella sakaiensis. Biochem Biophys Res Commun. 2019;508(1):289–94. https://doi.org/10.1016/j.bbrc.2018.11.148.
2. Rex Whinfield J, Tennant Dickson J. 'Polymeric Linear Terephthalic Esters', *Public Law*, vol. 1, pp. 1–7, 1945, [Online]. Available: https://www.google.com/patents/US2465319
3. Wyeth NC, Pa. Mendenhall, and, Roseveare RN. 'Biaxially oriented poly(ethylene terephthalate) bottle', *United State Patent Office*, pp. 1–6, 1973.
4. Zhang F, et al. Current technologies for plastic waste treatment: a review. J Clean Prod. 2021;282:124523. https://doi.org/10.1016/j.jclepro.2020.124523.
5. Thomsen TB, Almdal K, Meyer AS. 'Significance of poly(ethylene terephthalate) (PET) substrate crystallinity on enzymatic degradation', *N Biotechnol*, vol. 78, no. August 2023, pp. 162–172, 2023, https://doi.org/10.1016/j.nbt.2023.11.001
6. Wojnowska-Baryła K, Bernat, Zaborowska M. Plastic Waste Degradation in Landfill conditions: the Problem with Microplastics, and their direct and Indirect Environmental effects. Int J Environ Res Public Health. Oct. 2022;19(20). https://doi.org/10.3390/ijerph192013223.
7. Lamtai S, Elkoun M, Robert F, Mighri, Diez C. 'Mechanical Recycling of Thermoplastics: A Review of Key Issues', *Waste*, vol. 1, no. 4, pp. 860–883, Oct. 2023, https://doi.org/10.3390/waste1040050
8. Babaei M, Jalilian M, Shahbaz K. Chemical recycling of polyethylene terephthalate: a mini-review. J Environ Chem Eng. p. Mar. 2024;112507. https://doi.org/10.1016/j.jece.2024.112507.
9. Tournier V, et al. An engineered PET depolymerase to break down and recycle plastic bottles. Nature. 2020;580(7802):216–9. https://doi.org/10.1038/s41586-020-2149-4.
10. Soong YHV, Sobkowicz MJ, Xie D. 'Recent Advances in Biological Recycling of Polyethylene Terephthalate (PET) Plastic Wastes', Mar. 01, 2022, *MDPI*. https://doi.org/10.3390/bioengineering9030098
11. Maurya A, Bhattacharya, Khare SK. 'Enzymatic remediation of polyethylene terephthalate (PET)–Based polymers for Effective Management of Plastic Wastes: an overview', Nov. 19, 2020. Front Media S A https://doi.org/10.3389/fbioe.2020.602325
12. Soong YHV et al. Dec., 'Enzyme selection, optimization, and production toward biodegradation of post-consumer poly(ethylene terephthalate) at scale', *Biotechnol J*, vol. 18, no. 12, 2023, https://doi.org/10.1002/biot.202300119
13. Ronkvist ÅM, Xie W, Lu W, Gross RA. 'Cutinase-Catalyzed hydrolysis of poly(ethylene terephthalate)', *Macromolecules*, vol. 42, no. 14, pp. 5128–5138, Jul. 2009, https://doi.org/10.1021/ma9005318
14. Wei R, Song C, Gräsing D. and 'Conformational fitting of a flexible oligomeric substrate does not explain the enzymatic PET degradation', *Nat Commun*, vol. 10, no. 5581, Dec. 2019, [Online]. Available: https://doi.org/10.1038/s41467-019-13492-9
15. Müller RJ, Schrader H, Profe J, Dresler K, Deckwer WD. 'Enzymatic degradation of poly(ethylene terephthalate): Rapid hydrolyse using a hydrolase from T. fusca', *Macromol Rapid Commun*, vol. 26, no. 17, pp. 1400–1405, Sep. 2005, https://doi.org/10.1002/marc.200500410
16. Wei R et al. Aug., 'Engineered bacterial polyester hydrolases efficiently degrade polyethylene terephthalate due to relieved product inhibition', *Biotechnol Bioeng*, vol. 113, no. 8, pp. 1658–1665, 2016, https://doi.org/10.1002/bit.25941
17. Sonnendecker C et al. May., 'Cover Feature: Low Carbon Footprint Recycling of Post-Consumer PET Plastic with a Metagenomic Polyester Hydrolase (ChemSusChem 9/2022)', *ChemSusChem*, vol. 15, no. 9, 2022, https://doi.org/10.1002/cssc.202200696
18. Richter PK, et al. Structure and function of the metagenomic plastic-degrading polyester hydrolase PHL7 bound to its product. Nat Commun. Dec. 2023;14(1). https://doi.org/10.1038/s41467-023-37415-x.
19. Tiong E, et al. Expression and engineering of PET-degrading enzymes from Microbispora, Nonomuraea, and Micromonospora. Appl Environ Microbiol. 2023;89(11). https://doi.org/10.1128/aem.00632-23.
20. Van Gemeren A, Beijersbergen A, Van Den Hondel CAMJJ, Verrips CT. Expression and secretion of defined cutinase variants by aspergillus awamori. Appl Environ Microbiol. 1998;64(8):2794–9.
21. Wang X, Song C, Qi Q, Zhang Y, Li R, Huo L. Biochemical characterization of a polyethylene terephthalate hydrolase and design of high-throughput screening for its directed evolution. Eng Microbiol. Jun. 2022;2(2). https://doi.org/10.1016/j.engmic.2022.100020.
22. Sulaiman S, et al. Isolation of a novel cutinase homolog with polyethylene terephthalate-degrading activity from leaf-branch compost by using a metagenomic approach. Appl Environ Microbiol. 2012;78(5):1556–62. https://doi.org/10.1128/AEM.06725-11.
23. Seo H, Kim S, Son HF, Sagong HY, Joo S, Kim KJ. Production of extracellular PETase from Ideonella sakaiensis using sec-dependent signal peptides in E. Coli. Biochem Biophys Res Commun. 2019;508(1):250–5. https://doi.org/10.1016/j.bbrc.2018.11.087.
24. Aer L, Jiang Q, Gul I, Qi Z, Feng J, Tang L. Overexpression and kinetic analysis of Ideonella sakaiensis PETase for polyethylene terephthalate (PET) degradation. Environ Res. Sep. 2022;212. https://doi.org/10.1016/j.envres.2022.113472.
25. Su L, Xu C, Woodard RW, Chen J, Wu J. 'A novel strategy for enhancing extracellular secretion of recombinant proteins in Escherichia coli', *Appl Microbiol Biotechnol*, vol. 97, no. 15, pp. 6705–6713, Aug. 2013, https://doi.org/10.1007/s00253-013-4994-7
26. Su L, Jiang Q, Yu L, Wu J. Enhanced extracellular production of recombinant proteins in Escherichia coli by co-expression with Bacillus cereus phospholipase C. Microb Cell Fact. Feb. 2017;16(1). https://doi.org/10.1186/s12934-017-0639-3.
27. Tan Y, Henehan GT, Kinsella GK, Ryan BJ. 'Extracellular secretion of a cutinase with polyester-degrading potential by E. coli using a novel signal peptide from Amycolatopsis mediterranei', *World J Microbiol Biotechnol*, vol. 38, no. 4, Apr. 2022, https://doi.org/10.1007/s11274-022-03246-z

28. Lu H, et al. Machine learning-aided engineering of hydrolases for PET depolymerization. Nature. Apr. 2022;604(7907):662–7. https://doi.org/10.1038/s41586-022-04599-z.
29. Bell EL et al. 'Directed Evolution of an Efficient and Thermostable PET Depolymerase', *Nat Catal*, vol. 5, pp. 673–681, 2022, [Online]. Available: https://doi.org/10.1038/s41929-022-00821-3
30. Son HF et al. Apr., 'Rational Protein Engineering of Thermo-Stable PETase from Ideonella sakaiensis for Highly Efficient PET Degradation', *ACS Catal*, vol. 9, no. 4, pp. 3519–3526, 2019, https://doi.org/10.1021/acscatal.9b00568
31. Sagong HY, et al. Structural and functional characterization of an auxiliary domain-containing PET hydrolase from Burkholderiales bacterium. J Hazard Mater. May 2022;429. https://doi.org/10.1016/j.jhazmat.2022.128267.
32. Pirillo V, Orlando M, Battaglia C, Pollegioni L, Molla G. 'Efficient polyethylene terephthalate degradation at moderate temperature: a protein engineering study of LC-cutinase highlights the key role of residue 243', *FEBS Journal*, vol. 290, no. 12, pp. 3185–3202, Jun. 2023, https://doi.org/10.1111/febs.16736
33. Rosano GL, Ceccarelli EA. 'Recombinant protein expression in Escherichia coli: advances and challenges', 2014. Front Res Foundation. https://doi.org/10.3389/fmicb.2014.00172
34. Stargardt P, Feuchtenhofer L, Cserjan-Puschmann M, Striedner G, Mairhofer J. 'Bacteriophage Inspired Growth-Decoupled Recombinant Protein Production in Escherichia coli', *ACS Synth Biol*, vol. 9, no. 6, pp. 1336–1348, Jun. 2020, https://doi.org/10.1021/acssynbio.0c00028
35. Stargardt P, Striedner G, Mairhofer J. Tunable expression rate control of a growth-decoupled T7 expression system by l-arabinose only. Microb Cell Fact. Dec. 2021;20(1). https://doi.org/10.1186/s12934-021-01512-7.
36. Wei S-Q, Staders J. 'Distinct Regions of the LamB Signal Sequence Function in Different Steps in Export', *Journal of Biological Chemistry*, vol. 269, no. 3, pp. 1648–1653, 1994, [Online]. Available: https://doi.org/10.1016/S0021-9258(17)42076-X
37. Zhang YB, Howitt J, McCorkle S, Lawrence P, Springer K, Freimuth P. 'Protein aggregation during overexpression limited by peptide extensions with large net negative charge', *Protein Expr Purif*, vol. 36, no. 2, pp. 207–216, Aug. 2004, https://doi.org/10.1016/j.pep.2004.04.020
38. Köppl C, et al. Fusion Tag Design influences Soluble recombinant protein production in Escherichia coli. Int J Mol Sci. Jul. 2022;23(14). https://doi.org/10.3390/ijms23147678.
39. O'Shannessy DJ, O'Donnell KC, Martin J, Brigham-Burke M. 'Detection and quantitation of hexa-histidine-tagged recombinant proteins on western blots and by a surface plasmon resonance biosensor technique', *Analytical Biochemistry*, vol. 229, pp. 119–124, Jul. 1195, https://doi.org/10.1006/abio.1995.1387
40. Mason B, et al. Expression, purification, and characterization of recombinant nonglycosylated human serum transferrin containing a C-terminal hexahistidine tag. Protein Expr Purif. 2001;23(1):142–50. https://doi.org/10.1006/prep.2001.1480.
41. Summers DK. Sherratt1, 'Resolution of ColE 1 dimers requires a DNA sequence implicated in the three-dimensional organization of the cer site'. EMBO J. 1988;7(3):851–8.
42. Kastenhofer J, Rettenbacher L, Feuchtenhofer L, Mairhofer J, Spadiut O. Inhibition of E. Coli host RNA polymerase allows efficient extracellular recombinant protein production by enhancing outer membrane leakiness. Biotechnol J. Mar. 2021;16(3). https://doi.org/10.1002/biot.202000274.
43. Ho NHE, et al. Heterologous expression and characterization of Aquabacterium parvum lipase, a close relative of Ideonella sakaiensis PETase in Escherichia coli. Biochem Eng J. Aug. 2023;197. https://doi.org/10.1016/j.bej.2023.108985.
44. Papaneophytou CP. G. Kontopidis 2014 Statistical approaches to maximize recombinant protein expression in Escherichia coli: a general review. Acad Press Inc https://doi.org/10.1016/j.pep.2013.10.016.
45. Ravitchandirane G, Bandhu S, Chaudhuri TK. Multimodal approaches for the improvement of the cellular folding of a recombinant iron regulatory protein in E. Coli. Microb Cell Fact. Dec. 2022;21(1). https://doi.org/10.1186/s12934-022-01749-w.
46. Messens J, Collet JF. 'Pathways of disulfide bond formation in Escherichia coli', 2006. https://doi.org/10.1016/j.biocel.2005.12.011
47. Kadokura H, Katzen F, Beckwith J. 'Protein Disulfide bond Formation Prokaryotes'. 2003. https://doi.org/10.1146/annurev.biochem.72.121801.161459.
48. Yoshida S et al. Mar., 'A bacterium that degrades and assimilates poly(ethylene terephthalate)', *Science (1979)*, 2016, https://doi.org/10.1126/science.aad6359

Publisher's note